

# EFECTUL Cu ASUPRA PROPRIETĂȚILOR FIZICE ALE ZnO SINTETIZAT PRIN TEHNICA PULVERIZĂRII CU PIROLIZĂ EFFECT OF Cu ON THE PHYSICAL PROPERTIES OF ZnO SYNTHESIZED BY SPRAY PYROLYSIS TECHNIQUE

A. EL HAT \*, A. HADRI, F.Z. CHAFI, B. FARES, N. HASSANAIN , A. MZERD  
University Mohammed V, Faculty of Sciences, Physics Department, LPM, B.P. 1014, Rabat, Morocco

*Zn<sub>1-x</sub>Cu<sub>x</sub>O thin films with different Cu concentration x= (0; 2; 5; 7 at %) are deposited by spray pyrolysis technique on heated glass substrate at 350°C. The physical properties of the films are characterized by several techniques in order to study their structural, surface roughness, optical and electrical properties. It is observed from X-ray diffraction (XRD) analysis that the Cu doped ZnO films are polycrystalline and exhibit a preferential orientation along (002) plane. The Atomic force microscopy (AFM) measurements revealed that the surface roughness of the films is decreased from 0 to 5 at % Cu then increased strongly for 7 at % Cu. From optical measurements, a significant decrease in average optical transmission is observed for all doped samples and the band gap value is decreased from 3.3 to 3.07 eV with increase in Cu concentration. The Hall Effect electrical measurements show that all samples are n-type and the best value of the electrical resistivity 1.35x10<sup>-1</sup>(Ω.cm) is obtained for 5 at % Cu.*

**Keywords:** spray pyrolysis, ZnO thin films, Cu-doped ZnO, Hall Effect, Band gap, AFM, Refractive index, extinction coefficient

## 1. Introduction

Zinc oxide (ZnO) is a semiconductor with direct optical band gap ( $E_g = 3.37$  eV) and large exciton binding energy (60 meV) [1]. This band gap can be tuned in a range between 3.0 to 4.0 eV by doping with metals [2]. ZnO thin films have been widely investigated due to their advantageous aspects, such as low cost, non-toxicity, distinctive electronic, chemical properties and simplicity in fabrication [3]. These advantageous make it suitable for different applications such as gas sensors [4], optoelectronic [5], light emitting devices, futuristic spintronics devices [6] and solar cells [7]. For practical device applications, the proper dopants may be introduced into ZnO. Doping is a widely used method to improve physical properties of semiconductor compounds [5]. These properties can be greatly influenced by the chemical doping or formed intrinsic lattice defects. One of the efficient ways of improving the properties of ZnO films is the addition of certain impurities/ dopants. In particular, Among the different metallic doping elements Cu is important because, it has many physical and chemical properties that are similar to those of Zn such as the ionic radius of Cu<sup>2+</sup> (0.073 nm) which is similar to that of Zn<sup>2+</sup> ion (0.074 nm) [8], electronic shell structure, it is a prominent luminescence activator, which can modify the luminescence of ZnO crystals by creating localized impurity levels [3], and it can

change the microstructure and the optical properties of the ZnO system [9].

Cu-doped ZnO thin films have been synthesized by various techniques such as: direct current reactive magnetron sputtering [10], atomic layer deposition [11], hydrothermal [12-14], rough the vapor transport [15], magnetron co-sputtering [16], radio frequency sputtering [8], molecular beam epitaxy [17], chemical bath deposition [18], co-precipitation [6,7,9,19], one-step co-precipitating under atmospheric pressure [20], electrochemical (anodization) [21], sol-gel [22] and spray pyrolysis [2,3,23-27].

Until now, several physical and chemical techniques have been employed to prepare ZnO films which are more or less sophisticated and costly. Among these methods, the simple and inexpensive spray pyrolysis method allows easy control over deposition parameters as well as reproducibility [3].

However, exactly how copper sources affect the physical properties of CZO films has seldom been addressed. In this work the effect of Cu on the structure, optical and electrical properties of spray deposited ZnO films are investigated for its application in solar cells.

## 2. Experimental details

### 2.1 Sample preparation

Undoped and copper doped Zinc oxide (CZO) thin films are deposited onto heated glass substrates by

\* Autor corespondent/Corresponding author,  
E-mail: [abderrahim.elhat2012@gmail.com](mailto:abderrahim.elhat2012@gmail.com)

using the Spray pyrolysis technique. Starting with an aqueous solution containing the precursors such as zinc chloride  $ZnCl_2$  (0.05M) and copper chloride ( $CuCl_2, 2H_2O$ ) in distilled water at room temperature. Different solutions are prepared with different Cu concentration content (in the 0 – 7 at % Cu). The glass substrates are cleaned with ethanol, rinsed in distilled water, and subsequently dried. The substrates are then placed on a plate and heated progressively until the deposited temperature is reached. All films are deposited at  $350^\circ C$  during 80 min with a flow rate of the solution fixed at 2.5 ml/min. In spray unit, the substrate temperature is maintained with the help of a heater, controlled by a feedback circuit. After the spray, the substrate is naturally cooled down to  $50^\circ C$  and then removed from the spray station.

## 2.2 Characterization techniques

The X-ray diffraction (XRD) patterns of the samples are recorded using XRD with  $Cu_{K\alpha}$  radiation of wavelength  $\lambda=1.5406 \text{ \AA}$ , and scanning in a  $2\theta$  range from  $20^\circ$  to  $60^\circ$  by employing a Siemens D500 instrument. The morphology of the surfaces of the thin films is inspected by a Digital Instrument Dimension 3100 atomic force microscopy (AFM). The spectral optical transmission and reflectance are measured at normal incidence in UV-Vis spectral region (300–800 nm) with Lambda 900 UV/VIS/NIR Spectrometer. The electrical properties are investigated by ECOPIA Hall Effect instrument in the Van Der Pauw configuration at room temperature in air.

## 3. Results and discussion

### 3.1. Structural studies

Figure 1 shows the X-ray diffraction patterns of Cu doped ZnO thin films deposited for different Cu concentration. The peaks present (100), (002), (101), (102), and (110) correspond to hexagonal Wurtzite structure of ZnO. The peak at a Bragg's angle of  $\sim 34^\circ$ , which is attributed to the ZnO (002) plane, is dominantly observed for all samples. It is observed that the preferential orientation of the ZnO (002) peak obviously increased with increasing in Cu concentrations, which may be attributed to the influence arising from the difference in the ionic radius of  $Zn^{2+}$  (0.074 nm) and  $Cu^{2+}$  (0.073 nm) ions are different [8].

In order to study in some details these orientations, an analysis of the peak intensities has been done from the texture coefficient TCs (hkl) [26].

$$TC(hkl) = \frac{I_i(hkl)/I_0(hkl)}{n^{-1} \sum_{i=1}^n I_i(hkl)/I_0(hkl)} \quad (1)$$

Where  $I(hkl)$  and  $I_0(hkl)$  are the measured relative intensity of a plane (hkl) and standard intensity of

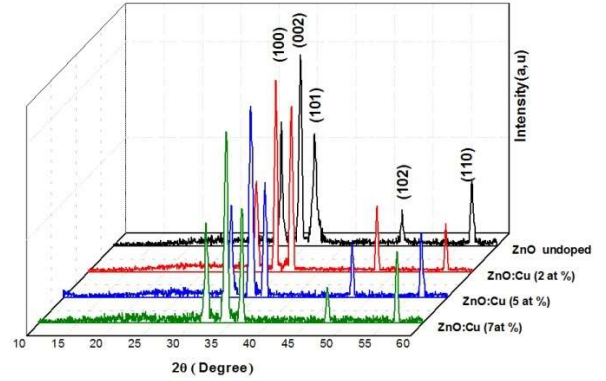


Fig.1 - XRD patterns of CZO sprayed thin films.

the plane (hkl) taken from JCPDS data [card No. 80-0075] respectively,  $n$  is the number of diffraction peaks. It is observed from Table.1 that the undoped and ZnO doped with Cu concentration have a very different TC coefficients for (100), (002) and (101) planes. Therefore, the films have a preferential orientation along the (002) direction and the amount of dopant did not change the preferential orientation in the deposited thin films.

The average crystallite size is approximately calculated by Scherrer formula [26]:

$$D = \frac{(0,9, \lambda)}{\beta, \cos\theta} \quad (2)$$

Where  $D$  is crystallite size,  $\lambda$  is X-ray wavelength (0.15406 nm),  $\beta$  is full width at half maximum, and  $\theta$  is diffraction angle. The (002) peaks are used to calculate the average crystallite size. From the table.1, it is observed that the average crystallite size  $D$  of the  $Zn_{1-x}Cu_xO$  films decreases with increasing Cu content, attains a minimum average crystallite size of about 20.2 nm for  $x=5\%$  at. To explain the shift of the peak related to ZnO:Cu toward large angles, we have calculated the lattice parameters, ( $a$ ) and ( $c$ ), of the films using XRD pattern with this relation [28]:

$$d_{hkl} = \frac{a}{\sqrt{\frac{4}{3}(h^2 + k^2 + hk) + l^2 \frac{a^2}{c^2}}} \quad (3)$$

Where  $h$ ,  $k$ , and  $l$  are the Miller indices, the lattice parameters  $a = 3.235\text{--}3.249 \text{ \AA}$  and  $c = 5.207\text{--}5.214 \text{ \AA}$  do not vary with dopant percent of Cu in solution. The lattices strain ( $\epsilon$ ) is calculated using the relation [9]:

$$\epsilon = \frac{\beta, \cos\theta}{4} \quad (4)$$

The values of dislocation densities ( $\delta$ ) are calculated using the relation [29,30]:

$$\delta = \frac{1}{D^2} \quad (5)$$

The lattice defects like micro-strain and dislocation density showed an increasing trend with increasing

Table.1

Various structural parameters of CZO sprayed thin films.

Samples	Thickness s (nm)	2θ value (Degree)	Tc(hkl)			Average crystallite size (D) (nm)	Cell parameter (Å)		ε (lattice strain)*10 <sup>-2</sup>	δ (dislocation densities) ligne/ m <sup>2</sup>
			(100)	(002)	(101)		a =b	c		
Undoped ZnO	638	34.42	0.830	1.742	0.426	21.886	3.235	5.207	0.158	3,608E+15
ZnO:Cu (2 at %)	455	34.4	0.614	1.765	0.620	20.791	3.239	5.210	0.166	3,996E+15
ZnO:Cu (5 at %)	416	34.36	0.661	1.872	0.465	20.282	3.245	5.216	0.170	4,195E+15
ZnO:Cu (7at %)	460	34.37	0.468	1.217	0.314	21.884	3.249	5.214	0.158	3,604E+15

doping concentration up to 5 at % and then decreased for further increase in doping concentration. The minimum values of ε and δ, which lead to the carriers to move freely in the lattice. It is generally observed that the strain and dislocation density in the film increases as the crystallite size decreases. We can conclude from the structural analysis that the Cu incorporation has little impact on the structural properties.

The micro-structural parameters like average crystallite size, lattice parameters, dislocation densities and strain have been calculated from the observed X-ray spectra. The thickness of the films has been found to be in the nanometer range using a stylus profilometer and the values are given in Table 1.

### 3.2 Atomic Force Microscopy (AFM)

Two dimensional and three dimensional micrographs of spray deposited CZO thin films on glass substrates at 350°C are recorded using AFM and the resulting micrographs are shown in Figure 2. These micrographs reveal that the formation of micro granular particles with spherical shaped and covered with grains of different sizes. The AFM analysis reveals that the film deposited at lower dopant concentrations has well defined grains, however, high dopant concentration (Cu-doped with 5 at %) lead to a more uniform and smoother surface.

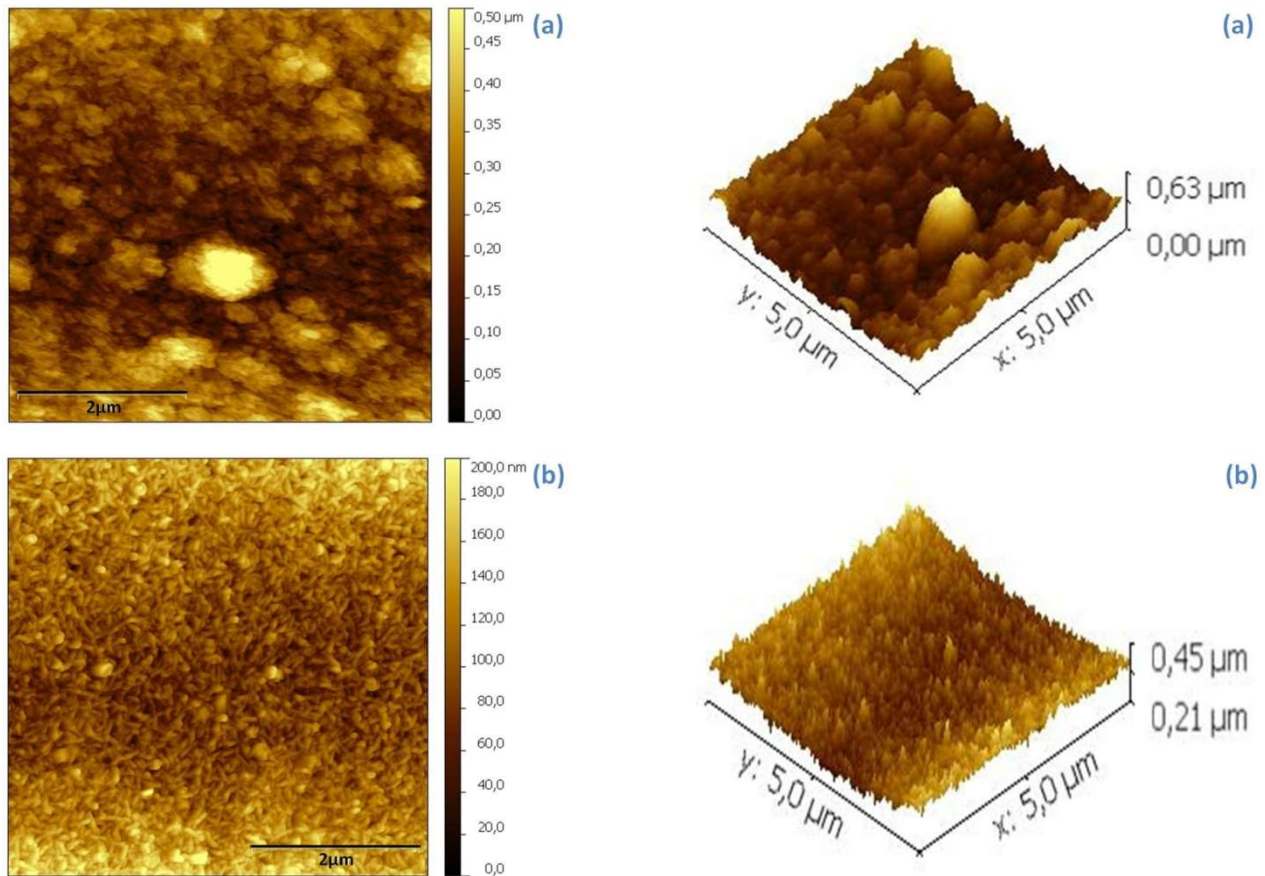


Fig. 2 continues on next page

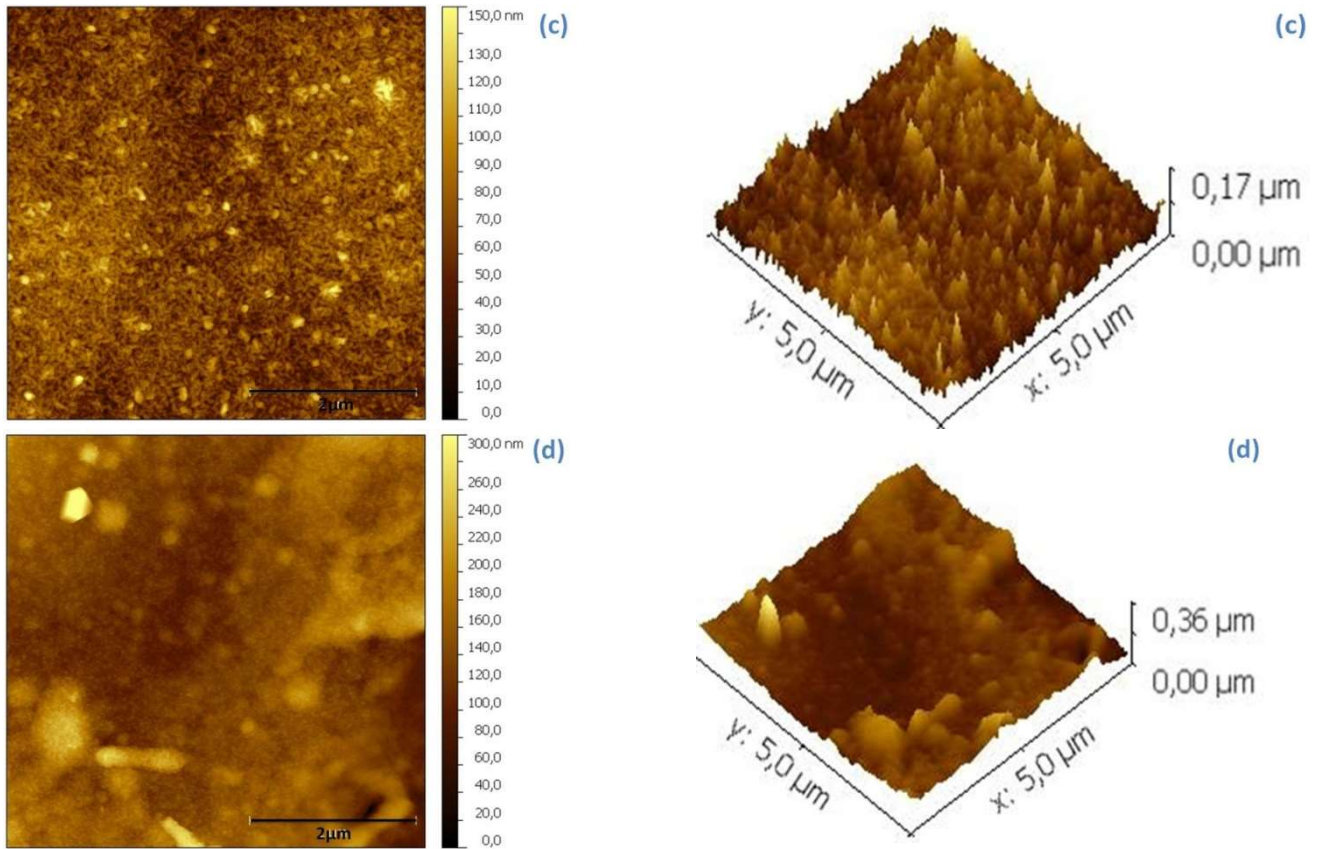


Fig.2 - AFM micrographs (5μm x 5μm) for (a) Undoped and Cu-doped (b) 2 at % (c) 5 at % (d) 7 at % ZnO films deposited at 350°C.

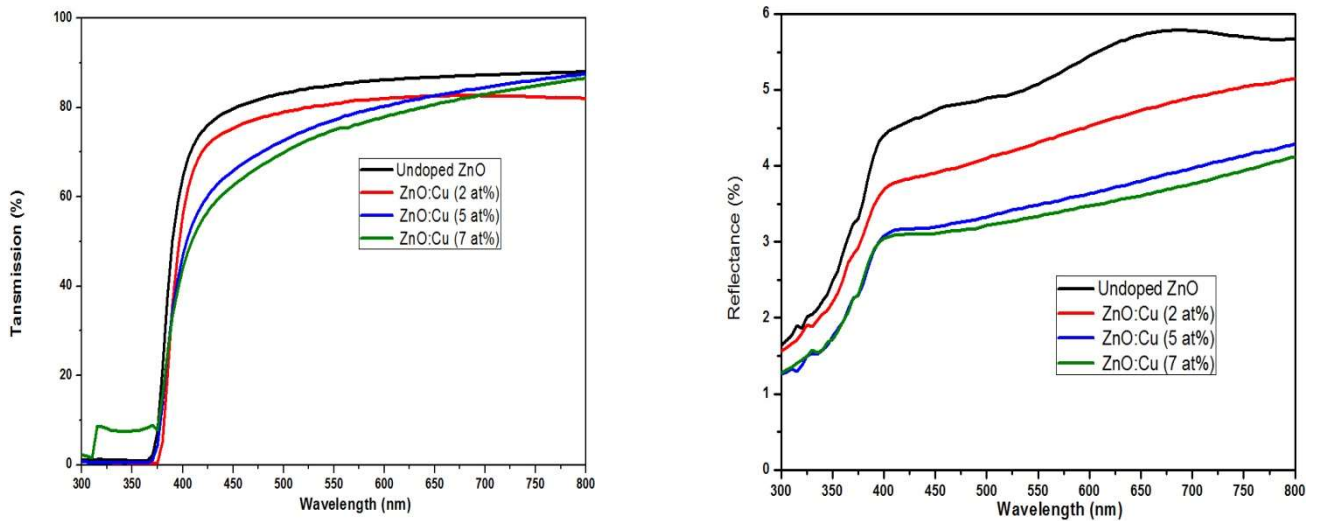


Fig. 3 - Transmission and reflectance spectra for Undoped and Cu-doped (0, 2, 5 and 7 at %) ZnO films prepared at 350°C.

The values of root mean square roughness (RMS) and mean roughness (Ra) of the layers depending on the Cu concentration are given in Table.2. We observe that , the ZnO layer Cu-doped with 5 at % has a low roughness value, root mean square (RMS) of about 32 nm, less than that of the ZnO layer undoped, which is approximately 86 nm.

This decrease in (RMS) surface roughness with an increase in Cu content in the CZO films occurred because the mean size of ZnO:Cu grains decreased with the amount of Cu dopant. Also, the surface topography of the films indicates that the grain growth is perpendicular to the substrate

Table 2

The average roughness RMS and Ra of the Cu-doped ZnO thin films

Samples	RMS (nm)	Ra (nm)
Undoped ZnO	86	68
ZnO:Cu (2 at %)	75	50
ZnO:Cu (5 at %)	32	27
ZnO:Cu (7at %)	82	69

surface [8]. On the other hand, the increase in RMS value for the sample doped with 7 at% Cu may be due to the agglomeration of crystallites.

### 3.3 Optical properties

Fig.3 shows the transmission and reflectance spectra of the sprayed CZO thin films in the wavelength range 300–800 nm. It is observed that the transmission is about 80% for undoped sample and decreases slightly with the increase in doping concentration due to increase of grain boundaries increases the light scattering, which in turn will lead to a decrease in transmission [31].

#### 3.3.1 Optical absorption coefficient ( $\alpha$ )

The optical absorption coefficient ( $\alpha$ ) is deduced from the optical transmission data using the following formula [32]:

$$\alpha = \frac{1}{d} \ln \left( \frac{100}{T(\%)} \right) \quad (6)$$

Where T is the optical transmission and d is the film thickness.

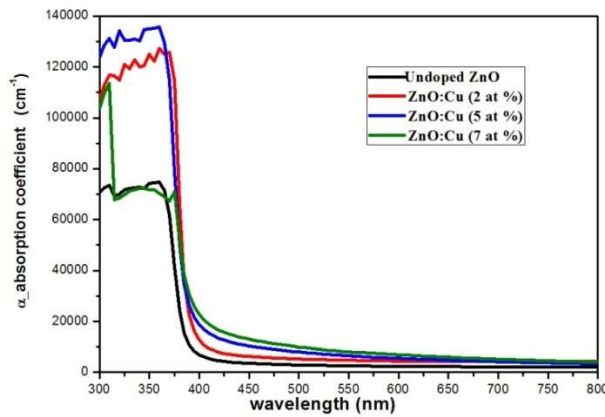


Fig.4 - The optical absorption coefficient.

The variation of the optical absorption coefficient  $\alpha$  with photon energy  $h\nu$  is shown in Figure 4 for undoped and doped ZnO thin films. It can be observed again around 380-390 nm. Below this wavelength, absorption coefficient increases with Cu concentration up to 5% of ZnO sample. It is observed that the highest absorption is obtained for the deposited layer at 5 % Cu. However, the observed decrease of the absorption coefficient (7% Cu) may be attributed to the slight increase of average crystallite.

#### 3.3.2. Energy band gap ( $E_g$ )

The optical band gap values ( $E_g$ ) are determined by using the relation [12]:

$$(\alpha h\nu)^2 = A[h\nu - E_g] \quad (7)$$

Where A is a constant, which is different for different transitions, h is the Planck's constant,  $\nu$  is the frequency of incident light, and  $E_g$  is the corresponding band gap.

From Figure 5, the band gaps values are determined as a function of Cu concentrations by extrapolating the straight line portion of the  $(\alpha h\nu)^2$

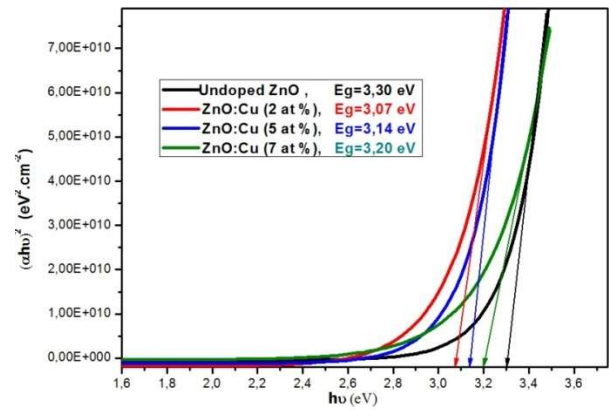


Fig.5 - Plots of  $(\alpha h\nu)^2$  versus  $h\nu$  for ZnO:Cu films with different values of Cu concentration.

versus  $(h\nu)$  variation to  $(\alpha h\nu)^2=0$ . The obtained values ranging from 0% to 7% are: 3.3 eV (ZnO), 3.07 eV ( $\text{Zn}_{0.98}\text{Cu}_{0.02}\text{O}$ ), 3.14 eV ( $\text{Zn}_{0.95}\text{Cu}_{0.05}\text{O}$ ), and 3.20 eV ( $\text{Zn}_{0.93}\text{Cu}_{0.07}\text{O}$ ). The band gaps are decreased due to the band shrinkage effect with increasing carrier concentration [8]. In addition, the band gaps are observed by Diouri et al. [33] and explained by the p–d spin-exchange interactions between the band electrons and the localized d electrons of the transition-metal ion substituting the  $\text{Cu}^{2+}$  ion. The reduction of band gap by Cu doping is also due to the strong p–d mixing of O and Cu [34]. These results indicate that the optical properties of ZnO films are affected by copper doping.

#### 3.3.3. Refractive index and extinction coefficient

The extinction coefficient is related to the absorption coefficient  $\alpha$  as [35]:

$$k = \frac{\alpha\lambda}{4\pi} \quad (8)$$

Where  $\lambda$  is the wavelength of incident light.

The refractive index is calculated at different wavelengths using the relation [25]:

$$n = \frac{1 + R^{1/2}}{1 - R^{1/2}} \quad (9)$$

Where, R is the optical reflectance.

The values of the refractive index (n) and the extinction coefficient (k) with wavelength for CZO thin films are shown in Figure 6. The effect of the Cu concentration on the sprayed ZnO films on all the optical parameters is prominent. From Fig.6 (a) it is observed that the refractive index is increased from 1.25 to 1.4 over the spectral range of 300–400 nm and then slowly increased to 1.65 for 800 nm of incident wavelength, but it decreases with increasing in Cu concentration. From the Figure 6 (b) it is clear that k decreases rapidly with the increasing wavelength from 390 nm to 800 nm. It is found that k values varying in the range of  $1.7 \times 10^{-3}$ – $3.9 \times 10^{-3}$ . The observed low extinction coefficient value of these films is a qualitative indication of surface softness and homogeneity of the films.

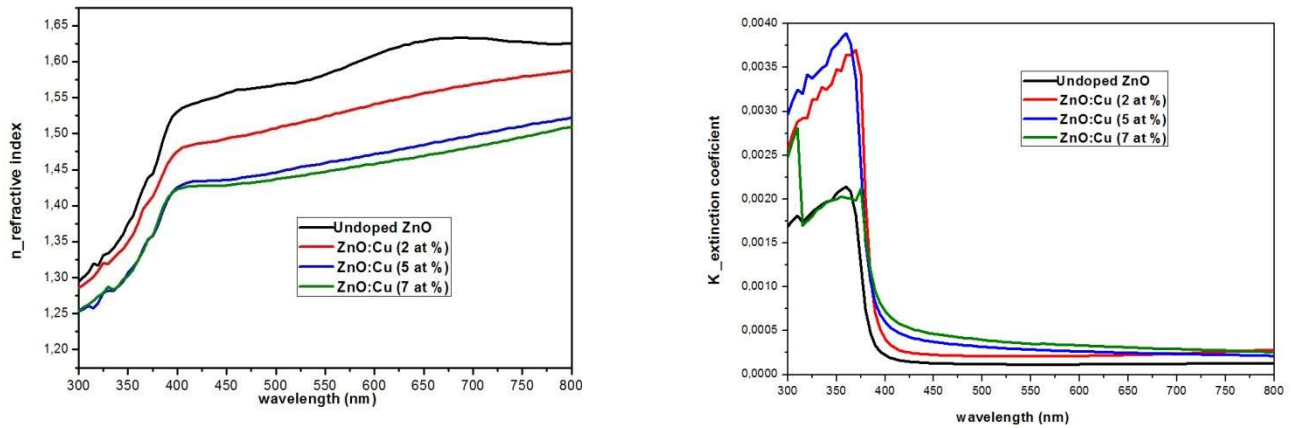


Fig.6. - Refractive index (a) and extinction coefficient (b) for ZnO:Cu films.

Table.3

Electrical resistivity of CZO sprayed thin films by sprat pyrolysis.

Samples	Resistivity $\rho$ ( $\Omega\text{cm}$ )	Mobility $\mu$ ( $\text{cm}^2\text{V}^{-1}\text{s}^{-1}$ )	Concentration ( $\text{cm}^{-3}$ )	Carrier type (Hall effect)
ZnO :Cu (0 % at)	9.41	9.23	$8.03 \times 10^{17}$	n
ZnO :Cu (2% at)	8.13	5.82	$1.17 \times 10^{18}$	n
ZnO :Cu (5 % at)	$1.35 \times 10^{-1}$	10.31	$7.44 \times 10^{19}$	n
ZnO :Cu (7 % at)	17.5	9.37	$3.78 \times 10^{16}$	n

### 3.4. The electrical properties

The carrier concentration  $n$ , the Hall mobility  $\mu$ , and the electrical resistivity  $\rho$ , of CZO thin films are measured by Hall measurement system at room temperature for the films deposited at various  $x$  concentration such as ( $x = 0; 2; 5; 7$  % at) and the results are given in Table 3. For undoped ZnO the obtained value is compared with that obtained after annealing of ZnO in Hydrogen atmosphere at  $150^\circ\text{C}$  [36]. For the films CZO, carriers originate from intrinsic donors by lattice defects and/or extrinsic doping. The minimum of electrical resistivity measured is  $1.35 \times 10^{-1} \Omega\text{.cm}$ , obtained for 5% of Cu and for 7 % it increases up to  $17.5 \Omega\text{.cm}$ . The valence state of Cu could be assumed to be +1 or/and +2 in the CZO films. The radii of  $\text{Cu}^+$ ,  $\text{Cu}^{2+}$  and  $\text{Zn}^{2+}$  ions were 0.096, 0.073 and 0.074 nm, respectively. So the  $\text{Cu}^+$ ,  $\text{Cu}^{2+}$  substitute and the  $\text{Cu}^{2+}$  interstitial might be the main impurities in the CZO film. Both  $\text{Cu}^+$  substitute and  $\text{Cu}^{2+}$  interstitial would affect the concentration of the interstitial Zn, oxygen vacancies and Zn vacancies [31,37]. As the doping level increased up to 5 % at, more dopant ions occupy the lattice interstitial, which results in more charge carriers. This process continues as long as the lattice interstitial is available. However, after a certain level of doping (at.Cu = 7 %), the Cu ions cannot occupy lattice interstitial. As a result, they form neutral defects and become ineffective as dopant impurities. All the samples showed n-type conductivity, indicating that the copper acts as a donor-type impurity.

### 4. Conclusions

The effect of copper doping on the properties of ZnO films deposited by spray pyrolysis technique is investigated. The XRD studies indicated that the films are polycrystalline in nature with preferred grain orientation along (002) plane and presented a hexagonal crystal structure. Due to copper doping, the crystallite size decreased from 21.8 nm to 20.2 nm. The film transmission value in the visible region is found to be above 80% and the optical band gap value decreased from 3.3 eV to 3.07 eV as doping concentration is increased. The optical and electrical studies clearly indicated the presence of Cu into ZnO. Hence the observed decreasing the optical band gap and the variation in electrical resistivity could be directly attributed to the effect of Cu ion incorporation into ZnO lattice. At 5 at.% Cu doping, the film has the lowest resistivity of  $1.35 \times 10^{-1} \Omega\text{.cm}$ . These CZO films may be used for photovoltaic devices.

### REFERENCES

1. T. M. Hammad, J. K. Salem, R. G. Harrison, R. Hempelmann, N. K. Hejazy, Optical and magnetic properties of Cu-doped ZnO nanoparticles, Journal of Materials Science: Materials in Electronics, 2013, **24**, 2846.
2. M. B. Rahmani, S. H. Keshmiri, M. Shafiee, K. Latham, W. Wlodarski, J. du Plessis, and K. Kalantar Zadeh, Transition fromn-top-Type of Spray Pyrolysis Deposited Cu Doped ZnO Thin Films for  $\text{NO}_2$  Sensing, Sensor Letters, 2009, **7**, 1.
3. P. S. Shewale, V.B. Patil, S.W. Shin, J.H. Kim, M.D. Uplanea,  $\text{H}_2\text{S}$  gas sensing properties of nanocrystalline Cu-doped ZnO thin films prepared by advanced spray pyrolysis, Sensors and Actuators B: Chemical, 2013, **186**, 226.

4. L. Chow, O. Lupan, G. Chai, H. Khallaf, L. K. Onoa, B. Roldan Cuenya, I. M. Tiginyanu, V.V. Ursakif, V. Sontea, A. Schulte, Synthesis and characterization of Cu-doped ZnO one-dimensional structures for miniaturized sensor applications with faster response, *Sensors and Actuators A: Physical*, 2013, **189**, 399.
5. A. Jagannatha Reddy, M. K. Kokila, H. Nagabhushana, R. P. S. Chakradhar, C. Shivakumara, J. L. Rao, B. M. Nagabhushana, Structural, optical and EPR studies on ZnO:Cu nanopowders prepared via low temperature solution combustion synthesis, *Journal of Alloys and Compounds*, 2011, **509**, 5349.
6. M. Ashokkumar, S. Muthukumar, Effect of Ni doping on electrical, photoluminescence and magnetic behavior of Cu doped ZnO nanoparticles, *Journal of Luminescence*, 2015, **162**, 97.
7. S. Singhal, J. Kaur, T. Namgyal, R. Sharma, Cu-doped ZnO nanoparticles: Synthesis, structural and electrical properties, *Physica B: Condensed Matter*, 2012, **407**, 1223.
8. N.E. Sung, S.W. Kang, H.J. Shin, H.K Lee, I.J. Lee, Cu doping effects on the electronic and optical properties of Cu-doped ZnO thin films fabricated by radio frequency sputtering, *Thin Solid Films*, 2013, **547**, 285.
9. S. Muthukumar, R. Gopalakrishnan, Structural, FTIR and photoluminescence studies of Cu doped ZnO nanopowders by co-precipitation method, *Optical Materials*, 2012, **34**, 1946.
10. D. L. Hou, X. J. Ye, H. J. Meng, H. J. Zhou, X. L. Li, C. M. Zhen, and G. D. Tang, Magnetic properties of n-type Cu-doped ZnO thin films, *Applied Physics Letters*, 2007, **90**, 142502.
11. S.S. Xu, H.L. Lu, Y. Zhang, T. Wang, Y. Geng, W. Huang, S.J. Ding, D.W. Zhang, Band gap narrowing and conductivity evolution of atomic-layer deposited ZnO:Cu thin films under rapid thermal annealing, *Journal of Alloys and Compounds*, 2015, **638**, 133.
12. M. Babikier, D. Wang, J. Wang, Q. Li, J. Sun, Y. Yan, Q. Yu and S. Jiao, Cu-doped ZnO nanorod arrays: the effects of copper precursor and concentration, *Nanoscale Research Letters*, 2014, **9**, 199.
13. C. Chen, W. Dai, Y. Lu, H. He, Q. Lu, T. Jin, Z. Ye, Origin of p-type conduction in Cu-doped ZnO nano-films synthesized by hydrothermal method combined with post-annealing, *Materials Research Bulletin*, 2015, **70**, 190.
14. J.L. Yu, Y.F. Lai, S.Y. Cheng, Q. Zheng, Y.H. Chen, Temperature-dependent photoluminescence and Raman investigation of Cu-incorporated ZnO nanorods, *Journal of Luminescence*, 2015, **161**, 330.
15. R. Mohan, K. Krishnamoorthy, S.J Kim, Enhanced photocatalytic activity of Cu-doped ZnO nanorods, *Solid State Communications*, 2012, **152**, 375.
16. Y. Liu, H. Liu, Y. Yu, Q. Wang, Y. Li, Z Wang, Structural and optical properties of ZnO thin films with heavy Cu-doping prepared by magnetron co-sputtering, *Materials Letters*, 2015, **143**, 319.
17. M. Suja, S. B. Bashar, M. M. Morshed, and J. Liu, Realization of Cu-Doped p-Type ZnO Thin Films by Molecular Beam Epitaxy, *ACS Applied Materials & Interfaces*, 2015, **7**, 8894.
19. A. Rahmati, A. B.Sirgani, M. Molaie, M. Karimpour, Cu-doped ZnO nanoparticles synthesized by simple co-precipitation route, *European Physical Journal Plus*, 2014, **129**, 250.
20. X. Wan, X. Liang, C. Zhang, X. Li, W. Liang, H. Xu, S. Lan, S. Tie, Morphology controlled syntheses of Cu-doped ZnO, tubular Zn(Cu)O and Ag decorated tubular Zn(Cu)O microcrystals for photocatalysis, *Journal of Chemical & Engineering*, 2015, **272**, 58.
21. B. El Filali, T.V. Torchynska, A.I. Diaz Cano, Photoluminescence and Raman scattering study in ZnO:Cu nanocrystals, *Journal of Luminescence*, 2015, **161**, 25.
22. Ian Yi-Yu Bu, Effect of Cu concentration on the structural and optoelectronic properties of ZnO:Cu:Al prepared by the sol-gel deposition method, *Ceramics International*, 2015, **41**, 4042.
23. L.C Chen, C.A Hsieh, X. Zhang, Electrical Properties of CZO Films Prepared by Ultrasonic Spray Pyrolysis, *Materials*, 2014, **7**, 7304.
24. R. K. Shukla, A. Srivastava, N. Kumar, A. Pandey and M. Pandey, Optical and Sensing Properties of Cu Doped ZnO Nanocrystalline Thin Films, *Journal of Nanotechnology* 2015, **2015**, 172864.
25. A. Hadri, B. Fares, A. Amari, M. Taibi, A. Mzerd, Transparent conducting Al and In codoped thin film deposited by spray pyrolysis, *Romanian Journal of Materials*, 2016, **46**, 63.
26. A. Hadri, M. Taibi, M. loughmarti, C.Nassiri, T. Slimani Tlemçani, A. Mzerd, Development of transparent conductive indium and fluorine co-doped ZnO thin films: Effect of F concentration and post-annealing temperature, *Thin Solid Films*, 2016, **601**, 7.
27. A. Hadri, M. Taibi, A. El hat, A. Mzerd, Transparent and conductive Al/F and In co-doped ZnO thin films deposited by spray pyrolysis *Journal of Physics: Conference Series*, 2016, **689**, 012024.
28. T. Prasada Rao, M.C. Santhoshkumar, Effect of thickness on structural, optical and electrical properties of nanostructured ZnO thin films by spray pyrolysis, *Applied Surface Science*, 2009, **255**, 4579.
29. A. Hadri, C. Nassiri, F. Z. Chafi, M. Loughmarti, A. Mzerd, Effect of Acetic Acid Adding on Structural, Optical and Electrical Properties of Sprayed ZnO Thin Films, *Energy and Environment Focus*, 2015, **4**, 12.
30. P. Sing, A. Kumar, A. Kaushal, D. Kaur, A. Pandey, RN. Goyal, In situ high temperature XRD studies of ZnO nanopowder prepared via cost effective ultrasonic mist chemical vapour deposition. *Bulletin of Materials Science*, 2008, **3**, 573.
31. X. Peng, J. Xu, H. Zang, B. Wang, Z. Wang, Structural and PL properties of Cu doped ZnO films, *Journal of Luminescence*, 2008, **128**, 297.
32. C.H. Hsu, L.C. Chen, X. Zhang, Effect of the Cu Source on Optical Properties of CuZnO Films Deposited by Ultrasonic Spraying, *Materials*, 2014, **7**, 1261.
33. J. Diouri, J.P. Lascaray, M. El Amrani, Effect of the magnetic order on the optical-absorption edge in  $Cd_{1-x}Mn_xTe$ , *Physical Review B*, 1985, **31**, 7995.
34. M. Ferhat, A. Zaoui, R. Ahuja, Magnetism and band gap narrowing in Cu-doped ZnO, *Applied Physics Letters*, 2009, **94**, 142502.
35. M.A. Majeed Khana, S. Kumar, M. Alhoshan, A.S. Al Dwayyan, Spray pyrolysed  $Cu_2ZnSnS_4$  absorbing layer: A potential candidate for photovoltaic applications, *Optics & Laser Technology*, 2013, **49**, 196.
36. J. Laube, D. Nübling, H. Beh, S. Gutsch, D. Hiller, M. Zacharias, Resistivity of atomic layer deposition grown ZnO: The influence of deposition temperature and post-annealing, *Thin Solid Films*, 2016, **603**, 377.
37. S.B. Zhang, S.H. Wei, A. Zunger, Intrinsic n-type versus p-type doping asymmetry and the defect physics of ZnO, *Physical Review B*, 2001, **63**, 075205.

\*\*\*\*\*